First arriving signals in layered waveguides. An approach based on dispersion diagrams

A. V. Shanin

January 8, 2016

Abstract

The first arriving signal (FAS) in a layered waveguide is investigated. It is well known that the velocity of such a signal is close to the velocity of the fastest medium in the waveguide, and it may be bigger than the fastest group velocity given by the dispersion diagram of the waveguide. Usually the FAS pulse decays with the propagation distance. A model layered waveguide is studied in the paper. It is shown that the FAS is associated with the pseudo-branch structure of the dispersion diagram. The velocity is determined by the slope of the pseudo-branch. The decay is exponential and it depends on the structure of the pseudo-branch. A new type of reference integral is introduced for FAS.

1 Introduction

Consider a layered 2D acoustic waveguide, which is homogenous in the x-direction and has a sandwich structure in the y-direction. The media constituting the waveguide can be elastic, liquid or gaseous. Waves in such a waveguide are described by a dispersion diagram in the (k, ω) coordinates (k is the wavenumber in the x-direction, ω is the temporal circular frequency). Usually the dispersion diagram is a graph consisting of several branches (curves). Each point of the dispersion diagram is characterized by two important parameters, namely by phase velocity $v_{\mathrm{p}} = \omega/k$ and group velocity $v_{\mathrm{g}} = d\omega/dk$ (the last one is the slope of the corresponding branch of

the dispersion diagram). It is well known that wave pulses propagate in the waveguide with corresponding group velocities.

It is well known also that in the experiment typically one can observe the *first arriving signal* (FAS) propagating with the velocity of the fastest medium in the structure of the waveguide. In the case of a single elastic isotropic medium the velocity of the FAS is close to the velocity of the longitudinal waves. In some cases the velocity of the FAS is bigger than any of the group velocities provided by the dispersion diagram. The FAS pulse decays with propagation distance unlike the pulses corresponding to usual modal pulses (the latter are called *guided waves* in the medical-related literature).

The most known applications of FAS are related to medical acoustics (see e.g. [1, 2]). A long bone can be considered as a tubular waveguide constituted of three media: a thin outer layer of dense (cortical) bone, a sponge bone underneath, and a liquid marrow core in the center. The fastest wave that can theoretically propagate in such media (taken separately as infinite spaces) is the longitudinal wave in the cortical bone. The sponge bone and the marrow bear much slower waves. However, when a standard analysis of a waveguide is performed (say, by the finite element method) the dispersion diagram contains no branch having group velocity close to the longitudinal cortical velocity. A standard interpretation of the FAS is [3], where this type of waves is treated as head waves. In [3] a thin cortical layer is substituted by an elastic half-space.

The author is not aware of a satisfying theory of the FAS propagation. The FAS can be interpreted as a head wave only for a very thick cortical layer. According to the concept of the first Fresnel zone, the thickness for which a layer can be replaced by a halfspace should be much bigger than $\sqrt{\lambda L}$, where λ is the wavelength of the fastest wave, and L is the propagation distance. For typical values of $\lambda = 1$mm, $L = 5$cm this thickness should be much bigger than 7mm, which is not typical. Moreover, the head wave model predicts a power decay, while a more refined model (see below) predicts an exponential decay.

The aim of the current paper is to present a model of FAS based on analysis of dispersion diagrams of a layered waveguide. It is known for a long time [4] that a wave process in a layered waveguide can be treated as an interaction between the modes of different types and velocities. Thus, the dispersion diagram has a "terrace-like" structure formed by overlapping of different sets of branches. Since typically no crossing of the branches can happen (except the branches corresponding to non-interacting waves),

there occur quasi-crossings at which the type of the mode is changing. A typical fragment of a dispersion diagram is shown in Fig. 1. Approximately, this diagram can be visually split into two sets of branches corresponding to fast waves (having big slope) and to a slow wave (having small slope). At each quasi-crossing the fast wave becomes slow and vice versa. The visible line of the biggest slope (although this line can be composed of segments corresponding to different branches, so it is a *pseudo-branch*) is related to the FAS. Fig. 1 displays a dispersion diagram of a model two-media acoustic waveguide studied in the paper.

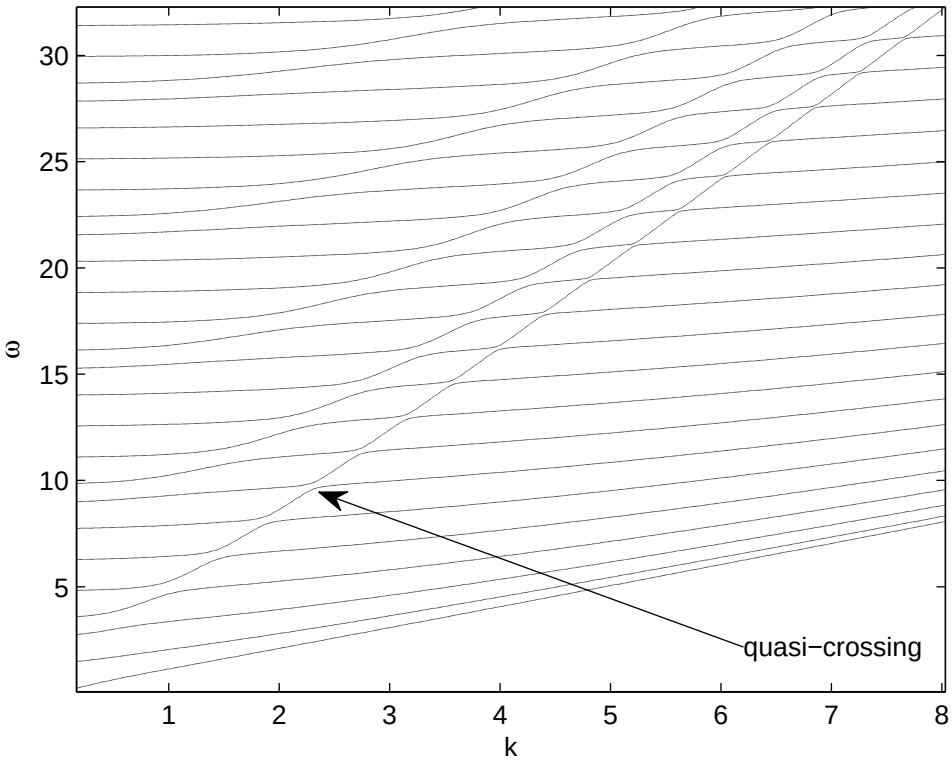

Fig. 1: A typical dispersion diagram

In the current paper this idea is developed into an analytical model. An approximation of a fragment of the dispersion diagram near the line of the biggest slope is constructed. A pulse shape is derived in the form of

a *reference integral*. A new type of reference integral is introduced for the studied case. The properties of the FAS pulse are derived from those of the reference integral.

To demonstrate that the model problem studied in the paper has a direct connection with more complicated practical problems, we plot in Fig. 2 a dispersion diagram for symmetrical Lamb waves for a material with the Poisson ratio $\sigma = 0.4$. The Young modulus and the density are equal to 1, the thickness is 2 (all parameters are dimensionless for simplicity).

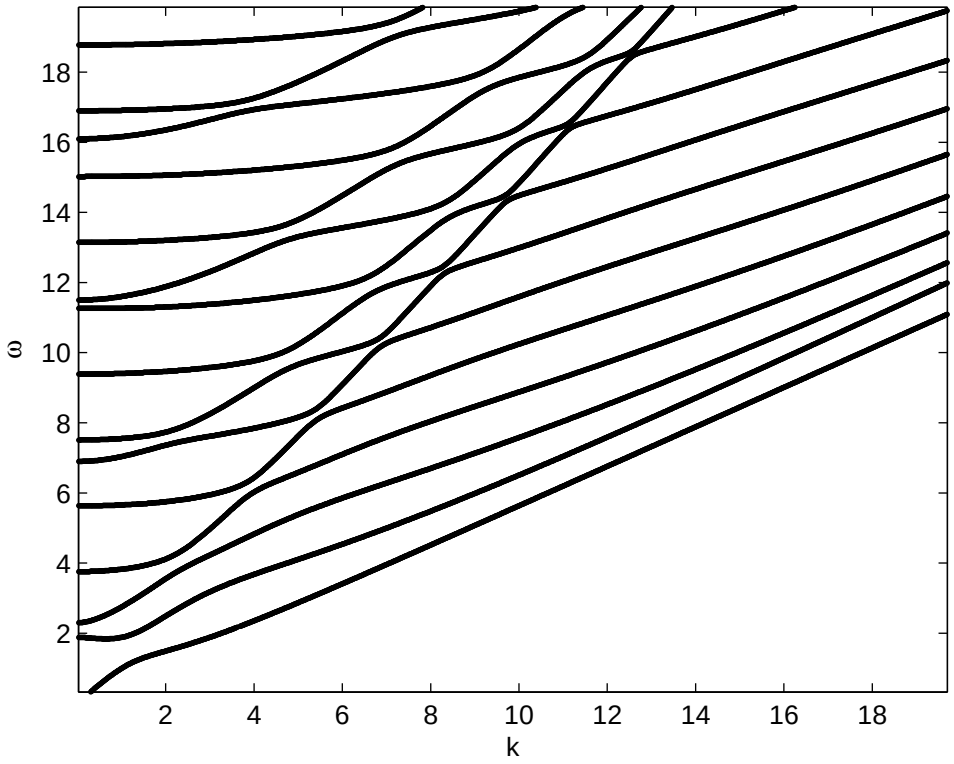

Fig. 2: A dispersion diagram for symmetrical Lamb waves

One can see a clear resemblance between Fig. 1 and Fig. 2. In both situations there are two types of waves (waves in different media in the first case, and shear / longitudinal waves in the second case). If the number of types of waves is bigger then the amount of sets of branches and pseudo-

branches is bigger, and the pattern is visually more complicated.

The structure of the paper is as follows. In Section 2 a model two-media problem is formulated. In Section 3 a numerical modeling of pulse propagation in the two-media problem is performed. The presence of FAS and its exponential decay are established. In Section 4 the signal in the waveguide is represented in the form of a reference integral. The reference integral is studied in Section 5.

2 A model waveguide

Consider a waveguide in the (x, y)-plane occupying the strip $-H_1 \le y \le H_2$ (see Fig. 3). The layer $H_1 \le y \le 0$ is filled with the medium having density and speed of sound equal to ρ_1, c_1, respectively. The layer $0 \le y \le H_2$ is filled with the medium with the parameters ρ_2, c_2. The wave equations in the media are as follows:

$$c_j^2(\partial_x^2 + \partial_y^2)u_j = \ddot{u}_j, \tag{1}$$

where $u_j(x, y, t)$, $j = 1, 2$ are the field variables (say, acoustical potentials), notation $\ddot{u}_j$ stands for the second time derivative.

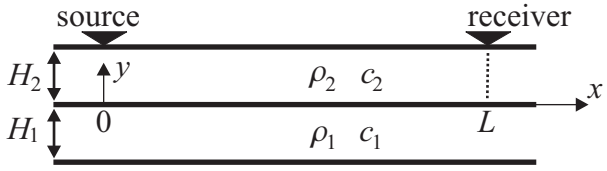

Fig. 3: Geometry of a model waveguide

The boundary conditions are as follows. The surface $y = -H_1$ is acoustically hard (Neumann):

$$\partial_y u_1(x, -H_1, t) = 0. \tag{2}$$

On the interface $y = 0$ the pressure and the normal velocity are continuous:

$$\rho_1 u_1(x, 0, t) = \rho_2 u_2(x, 0, t), \qquad \partial_y u_1(x, 0, t) = \partial_y u_2(x, 0, t). \tag{3}$$

The surface $y = H_2$ is acoustically hard, but a point source is located at the point $(0, H_2)$:

$$\partial_y u_2(x, H_2, t) = \delta(x) f(t), \tag{4}$$

where δ is the Dirac delta-function, $f(t)$ is the time shape of the probe pulse. The observation point is located at (L, H_2), i. e. the function $u_2(L, H_2, t)$ is recorded.

The problem of finding the signal on the receiver is quite standard and it can be solved easily. Namely, perform the Fourier transform of all variables in the time domain:

$$U_j(x, y, \omega) = \mathcal{F}_t[u_j(x, y, t)], \qquad F(\omega) = \mathcal{F}_t[f(t)], \tag{5}$$

where the direct and inverse Fourier transform in the time domain are given by the relations

$$\mathcal{F}_t[g(t)] = \int\limits_{-\infty}^{\infty} g(t)e^{i\omega t}dt, \qquad \mathcal{F}_t^{-1}[G(\omega)] = \frac{1}{2\pi}\int\limits_{-\infty}^{\infty} G(\omega)e^{-i\omega t}d\omega, \tag{6}$$

Then, perform the Fourier transform of U_j in the x-direction:

$$\tilde{U}_j(k, y, \omega) = \mathcal{F}_x[U_j(x, y, \omega)], \tag{7}$$

where

$$\mathcal{F}_x[g(x)] = \int\limits_{-\infty}^{\infty} g(x)e^{-ikx}dx, \qquad \mathcal{F}_x^{-1}[G(k)] = \frac{1}{2\pi}\int\limits_{-\infty}^{\infty} G(k)e^{ikx}dk. \tag{8}$$

Finally, get a 1D problem for $\tilde{U}_j(k, y, \omega)$ as functions of y. These functions should obey the equations

$$(\partial_y^2 + \alpha_j^2)\tilde{U}_1(k, y, \omega) = 0, \qquad \alpha_j = \alpha_j(k, \omega) = \sqrt{\frac{\omega^2}{c_j^2} - k^2}. \tag{9}$$

The following boundary conditions should be valid:

$$\partial_y\tilde{U}_1(k, -H_1, \omega) = 0, \qquad \partial_y\tilde{U}_2(k, H_2, \omega) = F(\omega), \tag{10}$$

$$\partial_y\tilde{U}_1(k, 0, \omega) = \partial_y\tilde{U}_2(k, 0, \omega), \qquad \rho_1\tilde{U}_1(k, 0, \omega) = \rho_2\tilde{U}_2(k, 0, \omega). \tag{11}$$

The solution of (9), (10), (11) can be found:

$$\tilde{U}_2(k, H_2, \omega) = F(\omega)\frac{M(k, \omega)}{N(k, \omega)}, \tag{12}$$

$$M(k,\omega) = \frac{\alpha_1}{\alpha_2}\sin(\alpha_1 H_1)\sin(\alpha_2 H_2) - \frac{\rho_1}{\rho_2}\cos(\alpha_1 H_1)\cos(\alpha_2 H_2), \tag{13}$$

$$N(k,\omega) = \alpha_2\frac{\rho_1}{\rho_2}\cos(\alpha_1 H_1)\sin(\alpha_2 H_2) + \alpha_1\sin(\alpha_1 H_1)\cos(\alpha_2 H_2). \tag{14}$$

The field on the receiver can be obtained by inverting the Fourier transformations:

$$u_2(x, H_2, t) = \frac{1}{4\pi^2}\iint\limits_{-\infty}^{\infty} F(\omega)\frac{M(k,\omega)}{N(k,\omega)}e^{ikx-i\omega t}dkd\omega \tag{15}$$

Formula (15) cannot be used directly, since zeros of the denominator belong to the plane of integration. The principle of limiting absorption helps to overcome this difficulty. Namely, for $\omega > 0$ we assume that the velocities c_j have vanishing *negative* imaginary parts, while for $\omega < 0$ the velocities c_j have vanishing *positive* imaginary parts. Due to this, for each ω the zeros of N in the complex k-plane become displaced from the real axis.

The dispersion diagram represents the zeros of $N(k,\omega)$ (for real c_j), i. e. the dispersion equation is

$$\frac{\alpha_1\tan(\alpha_1 H_1)}{\alpha_2\tan(\alpha_2 H_2)} = -\frac{\rho_1}{\rho_2}. \tag{16}$$

The roots of (16) are curves in the (k,ω) plane, each point of which corresponds to a wave freely propagating in the waveguide and having x- and t-dependence of the form $\exp\{i(kx-\omega t)\}$.

3 Numerical demonstration of FAS

The following parameters have been selected for a numerical demonstration of FAS presence: $H_1 = 1$, $H_2 = 0.4$, $c_1 = 1$, $c_2 = 5$, $\rho_1 = \rho_2 = 1$. The dispersion diagram for this waveguide is shown in Fig. 4. The fastest pseudo-branch is shown in the figure as a dash line. The pseudo-branch is composed of parts of real branches of the diagram. One can see that for the selected parameters the pseudo-branch is quite loose, i. e. the gaps between its parts are quite wide.

For the demonstration we are using the prrobe pulse $f(t)$ having the spectrum located in the part of the diagram shown in Fig. 4. Namely, we are using the region $20 < \omega < 40$. In this region the slopes of the branches, $d\omega/dk$, which are the group velocities of the guided waves, are smaller than 2.7. In

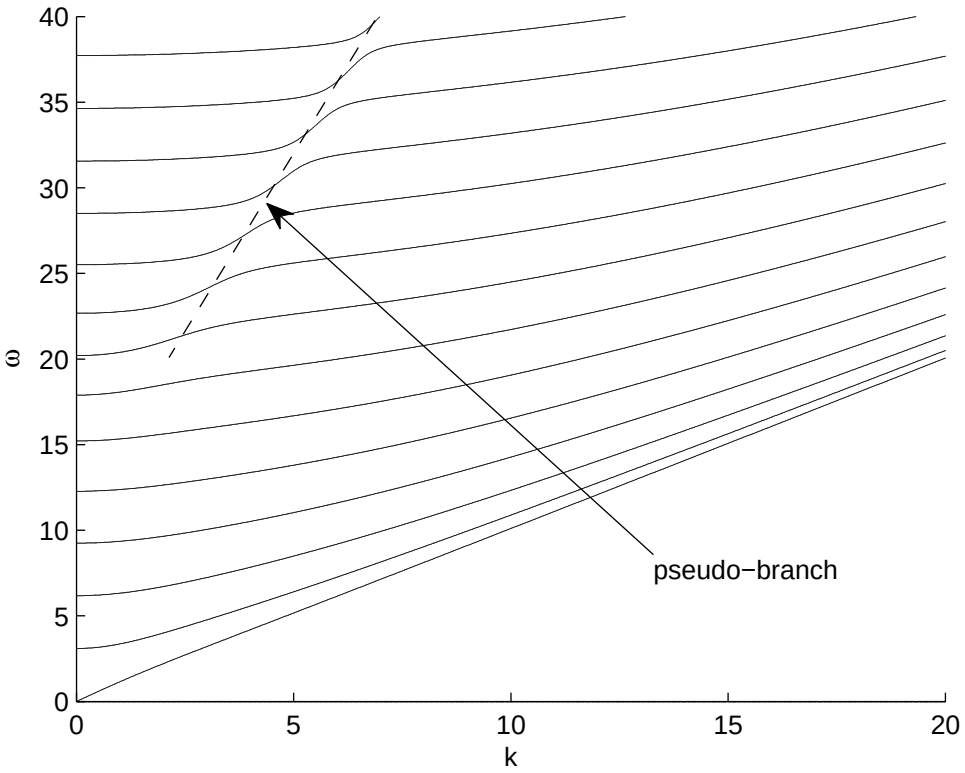

Fig. 4: A dispersion diagram for the waveguide with $H_1 = 1$, $H_2 = 0.4$, $c_1 = 1$, $c_2 = 5$, $\rho_1 = \rho_2 = 1$

the demonstration we are going to show the presence of a pulse whose velocity is approximately equal to the slope of the dashed line. This slope is equal to 4.3. The velocity of FAS will be considerably higher than that of any of the guided waves.

in Fig. 5 the shape of the pulse $f(t)$ (in the left) and the spectrum of this pulse (in the right) are shown. One can see that $f(t)$ is a radio pulse centered around $t = 0$. The central circular frequency is about $\omega_0 = 28$.

The results of the computations made by formula (15) for $L = 10, 20, 30$ are shown in Fig. 6, Fig. 7, Fig. 8, respectively. The field at the receiver, i. e. $u_2(L, H_2, t)$, is plotted. One can see that in all graphs there exists a small pulse, which can be interpreted as FAS.

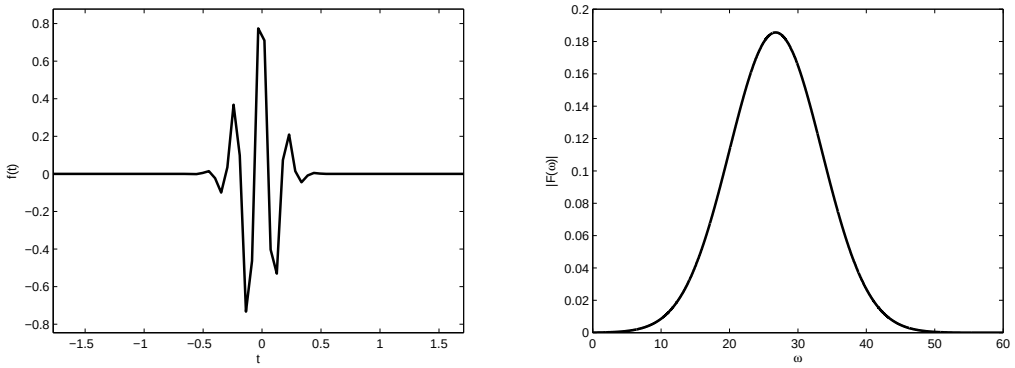

Fig. 5: Probing pulse $f(t)$ (left) and its spectrum (right)

Parameters of FAS approximately determined from these graphs are put into Table 1. ToF is the "time of flight", i. e. the travel time of FAS. One can see that the velocity of the pulse is more than 4, and the amplitude decay is close to exponential. Such a behavior is typical for FAS.

L	ToF	Amplitude
10	2.5	$1.8 \cdot 10^{-2}$
20	4.8	$2.5 \cdot 10^{-3}$
30	6.9	$5.0 \cdot 10^{-4}$

Table 1: Parameters of the FAS

4 Analysis of the dispersion diagram

Here our aim is to develop an analytical model of FAS. Transform the representation (15) by making some obvious simplifications. First, let function $f(t)$ be real. Consider the function

$$u_2'(x, H_2, t) = \frac{1}{4\pi^2} \int_0^\infty \int_{-\infty}^\infty F(\omega) \frac{M(k,\omega)}{N(k,\omega)} e^{ikx - i\omega t} dk d\omega, \tag{17}$$

i. e. exclude the negative values of ω. Obviously,

$$u_2(x, H_2, t) = 2\mathrm{Re}[u_2'(x, H_2, t)]. \tag{18}$$

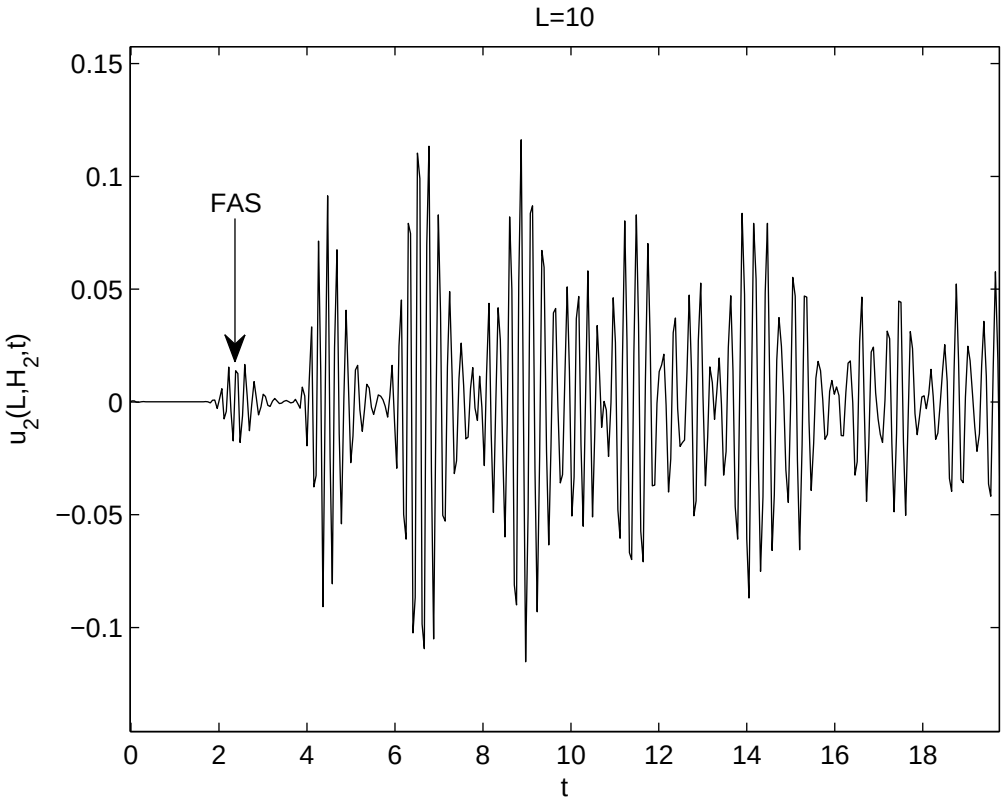

Fig. 6: Output pulse for L = 10

For each fixed positive ω find the roots of (16) by solving it as an equation with respect to k. Denote by $\xi_n(\omega)$ the roots having positive imaginary part or zero imaginary and positive real part. These roots correspond to waveguide modes traveling in the positive x-direction or decaying in this direction. Note that for for each $\omega > 0$ and for $x > 0$ the integral with respect to k in (17) can be considered as a contour integral, and the contour (the real axis) can be closed in the upper half-plane. The integrand is an meromorphic function in the upper half-plane, so the integral can be converted into a sum of residual terms:

$$u_2'(x, H_2, t) = \frac{i}{2\pi} \int_0^\infty F(\omega) \sum_n \frac{M(\xi_n(\omega), \omega)}{N'(\xi_n(\omega), \omega)} \exp\{i\xi_n(\omega)x - i\omega t\} d\omega, \qquad (19)$$

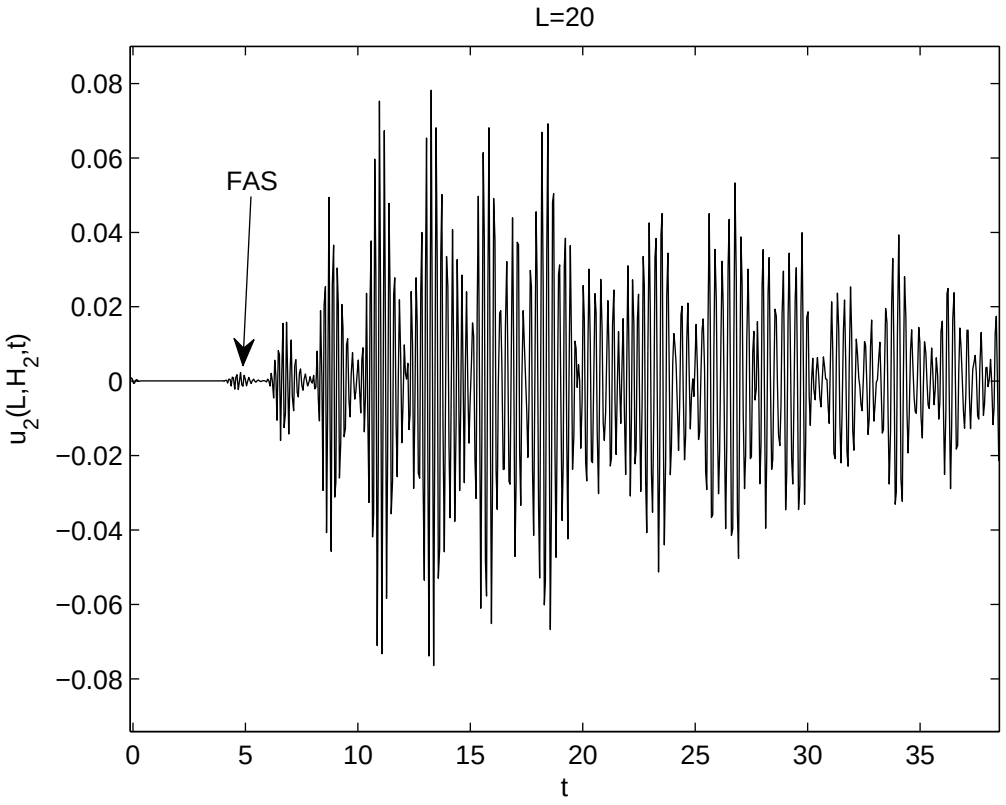

Fig. 7: Output pulse for L = 20

where

$$N'(k,\omega) = \partial_k N(k,\omega). \tag{20}$$

Of course, (19) is a standard expansion of the wave field in the waveguide as a sum of waveguide modes.

Let be $c_2 > c_1$. We are looking for the approximation the fastest pseudo-branch of the dispersion diagram, i. e. of the part of diagram lying in proximity of the line $\omega = kc_2$. The approximation should be valid near some point $\omega = \omega_0$, The vicinity of ω_0 in which the approximation is valid should be large enough to cover the temporal spectrum of the probing signal. We are looking for some parametric representation $\omega = \omega_*(\beta)$, $k = k_*(\beta)$ of the pseudo-branch. Since the pseudo-branch is composed of fragments of several branches, we are looking for functions $\omega_*(\beta)$, $k_*(\beta)$ which are discontinuous.

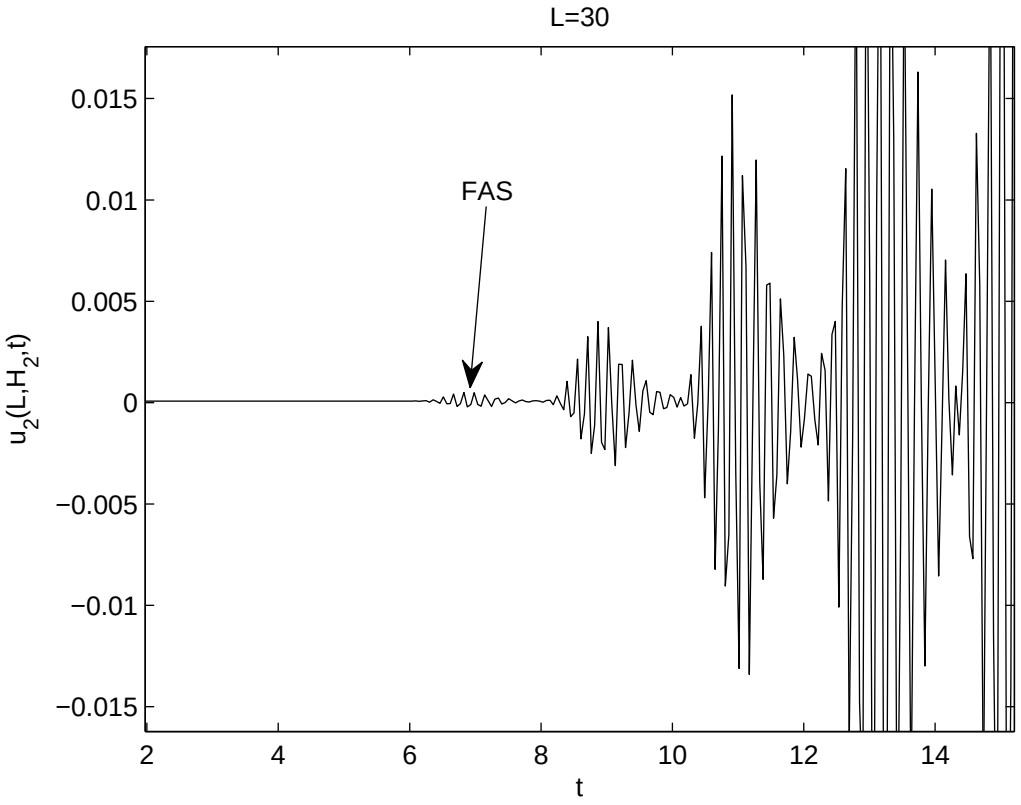

Fig. 8: Output pulse for L = 30

When functions $\omega_*(\beta)$, $k_*(\beta)$ are found they can be substituted into (19) providing a contribution corresponding to FAS:

$$u'_{\rm fas}(x, H_2, t) = \frac{i}{2\pi} \int\limits_0^\infty G(\beta) \exp\{ik_*(\beta)x - i\omega_*(\beta)t\} d\beta, \tag{21}$$

$$G(\beta) = F(\omega_*(\beta)) \frac{M(k_*(\beta), \omega_*(\beta))}{N'(k_*(\beta), \omega_*(\beta))} \frac{d\omega_*(\beta)}{d\beta}. \tag{22}$$

Consider a proximity of the point (k_0, ω_0). The frequency ω_0 is the central frequency of the probing pulse, the wavenumber k_0 will be defined later. Let be

$$\omega_* = \omega_0 + \Delta\omega, \qquad k_* = k_0 + \Delta k. \tag{23}$$

Perform a transformation of coordinates from the pair $(\Delta k, \Delta\omega)$ to the pair (ζ, β), where

$$\alpha_2(k,\omega) = \alpha_2(k_0,\omega_0) + \zeta, \qquad \alpha_1(k,\omega) = \alpha_1(k_0,\omega_0) + \beta. \tag{24}$$

In the linear approximation the transformation can be written in the matrix form

$$\begin{pmatrix} \Delta k \\ \Delta\omega \end{pmatrix} = J \cdot \begin{pmatrix} \zeta \\ \beta \end{pmatrix}, \tag{25}$$

where

$$J = \left(\frac{\partial(\zeta,\beta)}{\partial(\Delta k, \Delta\omega)}\right)^{-1} = \begin{pmatrix} -k_0/\alpha_2(k_0,\omega_0) & \omega_0/(c_2^2\alpha_2(k_0,\omega_0)) \\ -k_0/\alpha_1(k_0,\omega_0) & \omega_0/(c_1^2\alpha_1(k_0,\omega_0)) \end{pmatrix}^{-1}. \tag{26}$$

Direct computations yield

$$J = \left(c_1^{-2} - c_2^{-2}\right)^{-1} \begin{pmatrix} -\alpha_2(k_0,\omega_0)/(k_0c_1^2) & \alpha_1(k_0,\omega_0)/(k_0c_2^2) \\ -\alpha_2(k_0,\omega_0)/\omega_0 & \alpha_1(k_0,\omega_0)/\omega_0 \end{pmatrix} = \begin{pmatrix} J_{11} & J_{12} \\ J_{21} & J_{22} \end{pmatrix}. \tag{27}$$

An elementary analysis shows that the fastest pseudo-branch corresponds to

$$H_2\alpha_2 \approx \frac{\pi}{2}. \tag{28}$$

Therefore, we can take $\alpha_2(k_0,\omega_0) = \pi/(2H_2)$, and

$$k_0 = \sqrt{\frac{\omega_0^2}{c_2^2} - \frac{\pi^2}{(2H_2)^2}}, \qquad \alpha_1(k_0,\omega_0) = \sqrt{\frac{\omega_0^2}{c_1^2} - \frac{\omega_0^2}{c_2^2} + \frac{\pi^2}{(2H_2)^2}}. \tag{29}$$

The dispersion equation (16) can be approximately written in the form

$$\frac{\alpha_2(k_0,\omega_0)\tan(\pi/2 + H_2\zeta)}{\alpha_1(k_0,\omega_0)\tan(H_1(\alpha_0(k_0,\omega_0)+\beta))} \approx -\frac{\rho_2}{\rho_1}. \tag{30}$$

Note that

$$\tan(\pi/2 + H_2\zeta) \approx -\frac{1}{H_2\zeta}. \tag{31}$$

Thus, an approximate solution is as follows:

$$\zeta = \zeta(\beta) = -\frac{\rho_1}{H_2\rho_2}\frac{\alpha_2(k_0,\omega_0)}{\alpha_1(k_0,\omega_0)}\tan(H_1(\alpha_1(k_0,\omega_0)+\beta) + \pi/2). \tag{32}$$

Finally, the exponential factor in (21) can be rewritten as follows:

$$\exp\{i(k_*(\beta)x-\omega_*(\beta)x)\} = \exp\{i(k_0x-\omega_0t)\}\exp\{ia\tan(s\beta-r)-ib\beta\}, \quad (33)$$

where

$$a = A(J_{11}x - J_{21}t), \qquad A = -\frac{\rho_1}{H_2\rho_2}\frac{\alpha_2(k_0,\omega_0)}{\alpha_1(k_0,\omega_0)}, \quad (34)$$

$$b = J_{22}t - J_{12}x, \quad (35)$$

$$s = H_1, \quad (36)$$

$$r = -H_1\alpha_1(k_0,\omega_0) - \pi/2. \quad (37)$$

An illustration of the approximation of the dispersion diagram in the vicinity of the point (k_0, ω_0) is given in Fig. 9. The form of the approximated parametric curve is as follows:

$$\begin{pmatrix} k_*(\beta) \\ \omega_*(\beta) \end{pmatrix} = \begin{pmatrix} k_0 \\ \omega_0 \end{pmatrix} + J \cdot \begin{pmatrix} \zeta(\beta) \\ \beta \end{pmatrix}. \quad (38)$$

5 Analysis of the reference integral

The reference integrals is the main tool in diffraction theory. Typically, the reference integral has the integrand containing a non-exponential factor (*without* a large parameter) and an exponential factor (*with* a large parameter). There are many known types of reference integrals, say, a saddle-point integral, an end point integral, a saddle point with a pole integral etc (see e. g. [5]). Note that, unfortunately, in the rigorous understanding our integral (39) is not a classical reference integral, since its structure is not becoming simpler as $a \to \infty$. Thus, our reasoning can be treated as approximate, but not asymptotical.

Our aim is to estimate the integral of the form

$$I(a,b) = \int G(\beta)\exp\{i(a\tan(s\beta - r) - b\beta)\}d\beta \quad (39)$$

with real a, b, s, r. The integration is held over some real segment. Let $G(\beta)$ be analytical in some strip of the complex plane β surrounding the segment of integration, maybe except the points

$$\beta_j = \frac{\pi(j+1/2)+r}{s}, \qquad j \in \mathbb{Z}, \quad (40)$$

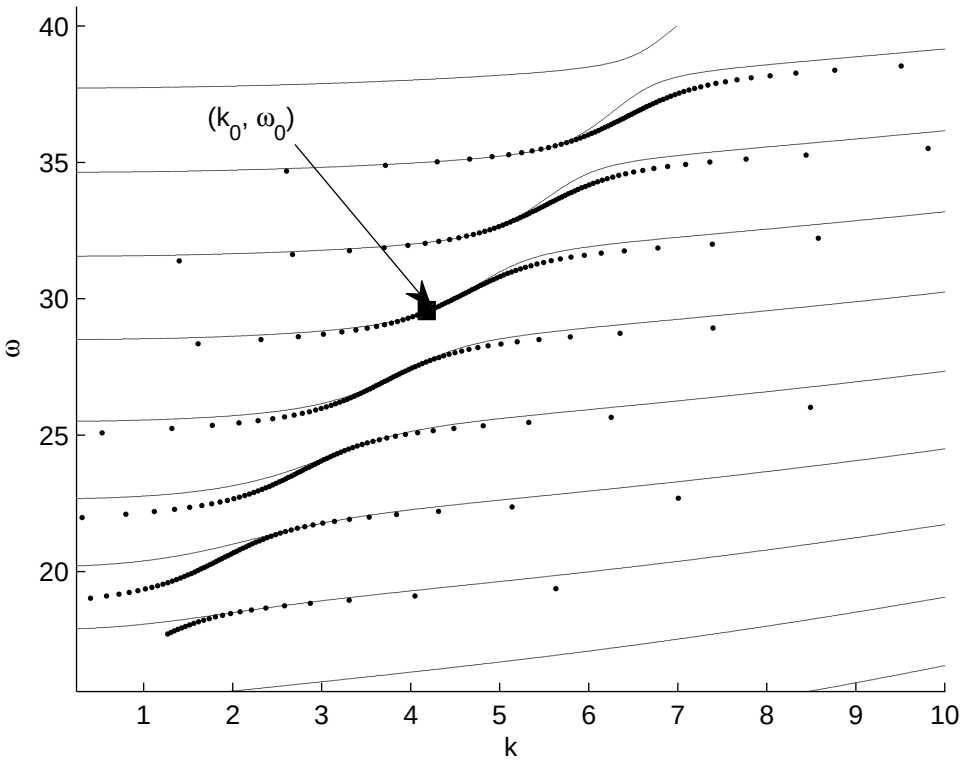

Fig. 9: Approximation of dispersion diagram by formulae (23), (29), (25), (32)

where it can have poles (these points are poles of the tangent function). Let the width of the strip of analyticity be much wider than $1/|s|$. Initially the integral should be treated as an improper integral on the segment with deleted points β_j.

Let a be positive. Transform the improper integral by adding small arcs about the points β_j (see Fig. 10, contour γ). Then transform the contour of integration into γ' (Fig. 10). The contour is shifted into the upper half-plane. The shift should be much bigger than $1/|s|$.

Note that

$$\tan(\phi) \to i \qquad \text{as} \qquad \mathrm{Im}[\phi] \to +\infty, \tag{41}$$

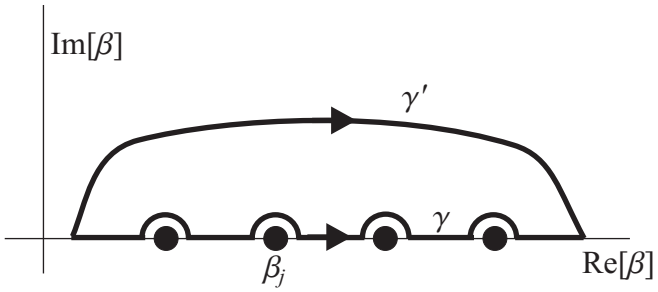

Fig. 10: Contour of integration for (39)

thus

$$I(a,b) \approx e^{-a} \int_{\gamma'} G(\beta) \exp\{-ib\beta\} d\beta = e^{-a} \int_{\gamma} G(\beta) \exp\{-ib\beta\} d\beta \qquad (42)$$

This formula gives the shape and the decay of the FAS pulse.

If $a < 0$ then contour γ should pass below the points β_j, and the contour γ' should be shifted into the lower half-plane. The exponential e^{-a} in (42) should be replaced by $e^{-|a|}$.

Finally, the integral is given by an approximate formula

$$I(a,b) \approx e^{-|a|} g(b), \qquad g(b) = \int_{\gamma} G(\beta) \exp\{-ib\beta\} d\beta. \qquad (43)$$

According to the form of b given by (35), the velocity of the pulse propagation is equal to

$$v_{\text{fas}} = \frac{J_{22}}{J_{12}}, \qquad (44)$$

i. e. to the slope of the dashed line in Fig. 4. Thus, one can take

$$x = L, \qquad t = \frac{L}{v_{\text{fas}}}, \qquad (45)$$

substitute them into (34) and get the decay in the form $\exp\{-|a|\} = \exp\{-\kappa L\}$,

$$\kappa = |A| \left| J_{11} - \frac{J_{21} J_{12}}{J_{22}} \right|. \qquad (46)$$

The parameters $v_{\text{fas}} = 4.3$ and $\kappa = 0.22$ observed in Table 1 correspond to frequency $\omega_0 = 33$, which is quite close to the central frequency of the pulse. Note that velocity and the decay determined by formulae (44) and (46) vary significantly within the spectrum of the probe pulse, so a more detailed study is necessary for a better description of wide-band FAS pulses.

6 Conclusion

It is shown that FAS pulses correspond to terrace-like structures of the dispersion diagrams. These structures are called pseudo-branches in the paper. A typical form of the pseudo-branch is shown in Fig. 4. The pulse propagation velocity for FAS is equal to the slope of the dashed curve in Fig. 4, and it can be bigger than any of the group velocities available in the considered part of the dispersion diagram.

To study the FAS pulse, the dispersion diagram in the vicinity of the pseudo-branch is approximated by a tangent function transformed by a linear (matrix) transformation (25). As the result, the integral is reduced to the form (39). The integral can be simplified by a shift of the integration contour. The decay of the pulse is provided by behavior of the tangent function in the complex plane. The pulse decays exponentially with the distance between the source and the receiver.

The analytical results agree reasonably with the numerical demonstration.

The work is supported by the grants RFBR 14-02-00573 and Scientific Schools-283.2014.2.

References

[1] M. Muller, P. Moilanen, E. Bossy, P. Nicholson, V. Kilappa, J. Timonen, M. Talmant, S. Cheng, and P. Laugier, Comparison of three ultrasonic axial transmission methods for bone assessment // Ultrs. Med. Biol. V. 31, pp. 633–642 (2005).

[2] J. Grondin, Q. Grimal, K. Engelke, and P. Laugier, Potential of first arriving signal to assess cortical bone geomtery at the hip with QUS: a model based study // Ultras. Med. Biol. V. 36, pp. 656–666 (2010).

[3] E. Camus, M. Talmsnt, G. Berger, and P. Laugier, Analysis of the axial transmission technique for the assessment of sceletal status // Journ. Acoust. Soc. Am., V. 108, pp. 3058–3065.

[4] R.D. Mindlin, Waves and vibrations in isotropic, elastic plates. In: Structural Mechanics. Eds J.N. Goodier and N. Hoff. Pergamon Press: New York, 1960. PP. 199–232.

[5] L.B. Felsen, N. Marcuwitz, Radiation and scattering of waves, Wiley-IEEE Press, 924p. (2001).